Volume II: Field Implementation of High-Volume Recycled Materials for Sustainable Pavement Construction

Authors:
Dr. Kamal H. Khayat, PhD, P.Eng.
Seyedhamed Sadati, PhD Candidate

DISCLAIMER

The contents of this report reflect the views of the authors, who are responsible for the facts and the accuracy of the information presented herein. This document is disseminated under the sponsorship of the U.S. Department of Transportation's University Transportation Centers Program, in the interest of information exchange. The U.S. Government assumes no liability for the contents or use thereof.
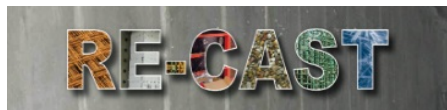
TECHNICAL REPORT DOCUMENTATION PAGE

1. Report No. RECAST UTC # 00046728	2. Government Accession No.	3. Recipient's Catalog No.
4. Title and Subtitle Volume II: Field Implementation of High-Volume Recycled Materials for Sustainable Pavement Construction		5. Report Date January 2020
		6. Performing Organization Code:
7. Author(s) Kamal H. Khayat and Seyedhamed Sadati		8. Performing Organization Report No. Project # 00046728
9. Performing Organization Name and Address RE-CAST – Missouri University of Science and Technology 500 W. 16th St., 223 ERL Rolla, MO 65409-0710		10. Work Unit No.
		11. Contract or Grant No. USDOT: DTRT13-G-UTC45
12. Sponsoring Agency Name and Address Office of the Assistant Secretary for Research and Technology U.S. Department of Transportation 1200 New Jersey Avenue, SE Washington, DC 20590		13. Type of Report and Period Covered: Final Report Period: 5/1/2014 – 12/31/2019
		14. Sponsoring Agency Code:

15. Supplementary Notes
The investigation was conducted in cooperation with the U. S. Department of Transportation.

16. Abstract
The objective of this study was to evaluate the feasibility of producing sustainable concrete materials for rigid pavement construction using high volume of recycled materials. The goal was to replace 50% of all solid materials in the concrete with recycled materials and industrial by-products. This included the replacement of cement with at least 50% supplementary cementitious materials (SCMs) and aggregate with 50% recycled concrete aggregate (RCA). Nine optimized mixtures from the first phase of the project that exhibited satisfactory performance were selected for the construction of single layer and two-lift rigid pavement systems. Life cycle cost assessment indicated that sustainable concrete with optimal SCMs and RCA can lead to cost savings of 17.6% of agency costs, 12.1% of user cost, 12.1% of social cost, and 17.5% of total life cycle cost. The development of a database and analysis using artificial intelligence was performed to quantify the properties of concrete as a function of RCA characteristics. Test results obtained through the case study indicated that the reduction in the modulus of elasticity (MOE) of pavement concrete can be limited to 10% when the coarse RCA has a water absorption lower than 2.5%, Los Angeles (LA) abrasion less than 23%, or oven dry specific gravity higher than 156 lb/ft3 (2500 kg/m3) for concrete made with 100% RCA replacement rate. The water absorption, specific gravity, and LA abrasion mass loss of RCA were found to categorize the RCA quality and resulting engineering properties of concrete made with RCA. The selection of RCA with a lower water absorption and LA abrasion mass loss and a higher oven dry specific gravity corresponded to a higher quality of RCA that can produce concrete with greater mechanical properties.

17. Key Words Concrete; Concrete pavements; Infrastructure; Paving; Recycled materials; Sustainable development	18. Distribution Statement No restrictions. This document is available to the public.	
19. Security Classification (of this report) Unclassified	20. Security Classification (of this page) Unclassified	21. No of Pages 59

Form DOT F 1700.7 (8-72)   Reproduction of form and completed page is authorized.

Field Implementation of High-Volume Recycled Materials for Sustainable Pavement Construction

Project Number: 2017-02
Final Report

Principal Investigator (PI): Dr. Kamal H. Khayat, Ph.D., P.Eng.

Seyedhamed Sadati, Ph.D.

ABSTRACT

The objective of this study was to evaluate the feasibility of producing sustainable concrete materials for rigid pavement construction using high volumes of recycled materials. The goal was to replace 50% of all solid materials in the concrete with recycled materials and industrial by-products. This included the replacement of cement with at least 50% supplementary cementitious materials (SCMs) and aggregate with 50% recycled concrete aggregate (RCA). Nine optimized mixtures from the first phase of the project that exhibited satisfactory performance were selected for the construction of single layer and two-lift rigid pavement systems. Life cycle cost assessment indicated that sustainable concrete with optimal SCMs and RCA can lead to cost savings of 17.6% of agency costs, 12.1% of user cost, 12.1% of social cost, and 17.5% of total life cycle cost. The development of a database and analysis using artificial intelligence was performed to quantify the properties of concrete as a function of RCA characteristics. Test results obtained through the case study indicated that the reduction in the modulus of elasticity (MOE) of pavement concrete can be limited to 10% when the coarse RCA has a water absorption lower than 2.5%, Los Angeles (LA) abrasion less than 23%, or oven dry specific gravity higher than 156 lb/ft^3 (2500 kg/m^3) for concrete made with 100% RCA replacement rate. The water absorption, specific gravity, and LA abrasion mass loss of RCA were found to categorize the RCA quality and resulting engineering properties of concrete made with RCA. The selection of RCA with a lower water absorption and LA abrasion mass loss and a higher oven dry specific gravity corresponded to a higher quality of RCA that can produce concrete with greater mechanical properties.

Keywords: Artificial intelligence; Life cycle cost analysis; Modulus of elasticity; Recycled concrete aggregate; Pavement construction; Sustainability

ACKNOWLEDGEMENT

TABLE OF CONTENTS

LIST OF FIGURES

LIST OF TABLES

1. INTRODUCTION

The decrease in natural resources and the growing problems associated with waste management, ecological hazards, and landfill limitations, as well as the increase in travel distance between natural resources and consumption markets support the idea of using recycled wastes for new concrete production (Padmini et al., 2009). Furthermore, the reduction in the carbon footprint of the most commonly used construction material, concrete, is a key factor to decrease the total greenhouse gas emissions produced by the construction industry (Mclntyre et al., 2009).

Interest in environmentally friendly concrete for pavement construction has grown in recent years. Candidate technologies to improve the sustainability of pavement concrete include the use of supplementary cementitious materials (SCMs) as a partial replacement for portland cement, the incorporation of recycled materials in concrete production, in particular recycled concrete aggregate (RCA), as well as the use of highly durable and crack-resistant materials. Due to the increasing rate of demolition, it is essential to reuse demolition wastes to conserve non-renewable natural resources, including aggregates for concrete. Given the fact that fine and coarse aggregates occupy about 30% and 40% of the concrete volume in rigid pavement, respectively, partial replacement of virgin aggregate with RCA can preserve natural resources and decrease the amount of disposals in landfills. Given the varied characteristics of RCA when compared to virgin aggregate sources, there still exists a conservative approach that limits the use of RCA in field implementations (Surya et al., 2013). Therefore, RCA is mostly being used in granular bases, embankments, sound barriers, and fills, etc. (Kim et al., 2013, Gabr and Cameron 2012).

Due to the economic and environmental merits of recycled materials, research has been undertaken to investigate the effect of RCA on the properties of concrete designated for pavement applications at Missouri University of Science and Technology (Missouri S&T) in collaboration

with the REsearch on Concrete Applications for Sustainable Transportation (RE-CAST) University Transportation Center (UTC) and the Missouri Department of Transportation (MoDOT). The project involves mixture design and field implementation of sustainable concrete materials made with high volumes of recycled materials for pavement applications. To date, field implementation was carried out by other consortium universities. The output of the project can endorse the development of guidelines for the design and construction of sustainable pavement applications.

The present report is composed of the following sections:

1. Literature review.

2. Laboratory investigation: summary of main findings from Phase I.

3. Field implementation.

4. Instrumentation.

5. Life cycle cost analysis - summary of findings from Phase I produced by the RE-CAST partner, Professor Kaan Ozbay, at New York University.

6. Artificial intelligence for investigating the effect of RCA on concrete properties - summary of the development of an extensive database and analysis of the effect of RCA physical prperties on the modulus of elasticity (MOE) of concrete. This work was conducted in collaboration with Professor Donald C. Wunsch from the Electrical Engineering Department at Missouri S&T.

2. LITERATURE REVIEW

A review of the literature on the use of RCA in concrete for the transportation infrastructure sector demonstrates the need to quantify the effect of using high-volume RCA on properties of pavement concrete. Of great interest was the use of at least 50% recycled materials in the construction of single-layer rigid pavement and the use of more than 50% recycled materials in two-lift rigid pavement systems.

2.1 USE OF RCA IN RIGID PAVEMENT CONSTRUCTION

Most of the applications of RCA in the U.S. involve the use of RCA as aggregate in base and subbase layers of pavement construction (FHWA 2004). Other applications include cement-treated base, backfill, embankment, stabilization, erosion control (riprap), and landscaping (ACPA 2009). According to a survey conducted by Garber et al. (2011), the use of RCA in new concrete production is rather advanced in European and East Asian countries. For example, in Finland, 10% of the RCA is used in new concrete mixtures or in cement-treated bases (Englesen et al., 2005). In Austria, RCA is mainly used for the production of the bottom layer in two-lift concrete pavement applications; however, it is also allowed for use in new concrete production for curbs and sidewalks.

The use of RCA in the construction of rigid pavements started in the early 1970s, and most of these pavements have performed well. However, several states in the U.S. stopped using RCA in pavement construction due to poor performance in some cases (Cuttell et al., 1997), which was associated with: (1) higher shrinkage and thermal deformation of RCA concrete, resulting in distress in mid-panel cracks of jointed reinforced concrete pavement (JRCP); (2) inferior load transfer along with faulting in non-doweled sections due to reduced aggregate interlock; (3)

durability issues, including delayed D-cracking due to use of RCA obtained from crushing of old concrete proportioned with aggregates that are highly susceptible to frost damage.

Cuttel et al. (1997) investigated the use of RCA for construction of single layer concrete pavements in the 1970s and 1980s in Connecticut (one section), Kansas (one section), Minnesota (four sections), Wisconsin (two sections), and Wyoming (one section). Jointed plain concrete pavements (JPCP), continuously reinforced concrete pavements (CRCP), and jointed reinforced concrete pavements (JRCPs) were investigated. Joint spacing ranged from 12 to 39 ft (3.7 to 12 m) and slab thicknesses varied between 7.9 and 11.0 in. (200 and 280 mm). The water-to-cementitious materials ratio (w/cm) of the investigated concrete mixtures ranged from 0.38 to 0.47. Based on core sample results, comparable compressive strength and splitting tensile strength values were found for the concrete sections made with or without RCA (Cuttel et al., 1997). The modulus of elasticity (MOE) results proved to be up to 18% lower than those of the control concrete. Up to 23% increase in coefficient of thermal expansion (CTE) was observed for the RCA-made sections. In addition, investigated sections had similar responses to falling weight deflection tests. However, inferior load transfer efficiency was observed in the case of RCA sections (Cuttel et al., 1997). The investigation was followed by a second survey in 2006 on the same sections that were 20- to 22-year old. Based on the field measurements and inspections, the authors reported an increase in transverse cracking and transverse joint spalling, increase in length of deteriorated transverse cracks, and decrease (up to 0.8 points out of 5.0) in present serviceability rating (PSR) of the pavement made with RCA.

Salas et al. (2010) used up to 100% RCA for producing concrete for rigid pavement applications as a part of the O'Hare Airport Modernization Project using the two-stage mixing approach developed by Tam et al. (2005). Compared to concrete made with virgin aggregate,

concrete prepared with RCA exhibited similar workability, lower bleeding and segregation, similar or higher compressive strength, and similar shrinkage at early age.

Choi and Won (2009) studied the performance of a CRCP highway section made with totally fine and coarse RCA mixtures located in Houston, TX. Based on core testing results, it was observed that the average compressive strength decreased due to the use of RCA. The MOE of the RCA concrete was lower than that of the virgin aggregate mixture. It is interesting to note that the CTE of the RCA concrete was similar to that of the virgin aggregate mixtures. The rapid chloride-ion permeability results of the RCA concrete were surprisingly lower than that of the virgin aggregate concrete and was rated as "very low" based on the ASTM C1202 (2012). The sulfate content of the RCA-made and the virgin aggregate mixtures were found to be similar. It was also reported that the RCA sections had overall good performance after more than 10 years of service life with no structural distress. The transverse crack distributions were also found to be similar to that of the virgin limestone mixtures (Choi and Won 2009).

2.2 RESEARCH NEED

In general, given the variable properties of RCA particles compared to the virgin aggregate sources, the mechanical properties and durability of concrete made with RCA may be lower than those of the conventional concrete made without any RCA. However, the degree of variation in results depends on the concrete composition and source of RCA. Laboratory screening is therefore required for the selection of RCA for the use in construction projects. Furthermore, a comprehensive test matrix is required to investigate the properties of concrete mixtures made with RCA for sustainable pavement construction. Based on the results published in the literature, as those summarized in the survey conducted in Phase I of this project, the following areas warrant further investigation:

- Key physical properties, including oven-dry specific gravity, water absorption, Los Angeles (LA) abrasion, presence of deleterious materials and degree of ionic contamination (chloride ions, sulfates, etc.) should be considered in categorizing RCA for various applications and environmental conditions.

- The content and quality of the selected RCA can reduce workability, specific gravity, mechanical properties, including compressive strength, splitting tensile strength, flexural strength, and MOE.

- Drying shrinkage can be significantly affected by the use of RCA. A greater content of RCA with lower quality can lead to higher shrinkage.

- Frost durability can be affected by the use of RCA that is produced from non-air entrained concrete or low-quality RCA. Carbonation, electrical resistivity, chloride ion permeability can also be affected by the use of RCA with high water absorption and/or contaminated with chloride ions.

3. LABORATORY INVESTIGATION

3.1 SUMMARY OF FINDINGS FROM PHASE I

A comprehensive laboratory investigation program was undertaken in the first phase of the project. Commercially produced RCA was used for developing and testing concrete mixtures, designated for single and double lift pavement constructions. Mixtures with desirable performance were selected. A summary of findings is provided below. The first phase of the laboratory investigation involved the evaluation of the properties of five sources of fine RCA and seven sources of coarse RCA for use in concrete production, as summarized in Table 1.

The aim of the research presented in this report was to evaluate the feasibility of producing sustainable concrete materials for rigid pavement construction using high volume of recycled materials. The goal was to replace 50% of the solids with recycled materials and industrial by-products. This included the use of at least 50% SCMs as cement replacement, as well as the incorporation of 50% RCA as a replacement for virgin aggregate.

Table 1 - Physical properties of investigated RCA sources

Aggregate	Specific gravity	Dry rodded unit weight (pcf)	Absorption (%)	Los Angeles abrasion (%)	Source
Fine RCA I	2.41	-	6.8	-	Lambert Airport, I
Fine RCA II	2.11	-	7.33	-	Lambert Airport, II
Fine RCA III	2.10	-	9.29	-	Commercial
Fine RCA IV	2.05	-	10.47	-	Commercial
Fine RCA V	1.90	-	14.19	-	Commercial
Coarse RCA I	2.38	91.0	4.2	33	Lambert Airport, I
Coarse RCA II	2.35	90.2	4.46	33	Lambert Airport, II
Coarse RCA III	2.21	86.1	6.66	43	Commercial
Coarse RCA IV	Rejected in visual inspection				Commercial
Coarse RCA V	2.32	88.4	4.99	35	Commercial
Coarse RCA VI	2.15	85.0	8.17	43	Commercial
Coarse RCA VII	2.35	89.7	4.56	41	Laboratory produced

Concrete equivalent mortar (CEM) based on MoDOT's portland cement concrete pavement (PCCP) mixture design was employed to optimize the binder composition of sustainable concrete pavement. The mixture designs of the base concrete and corresponding CEM are given in Table 2.

Table 2 - Mixture composition of base concrete and corresponding CEM mixtures (lb/yd^3)

	Cementitious materials	w/cm	Water content	Sand	Coarse aggregate	Coarse-equivalent sand
MoDOT PCCP	545	0.40	218	1265	1890	-
CEM	990	0.40	396	2275	-	305

A multi-criteria decision-making method was employed for the optimization of binary and ternary binder systems. The investigated properties and corresponding importance weights assigned to the various parameters were:

✓ Compressive strength, importance weight of 3;

✓ Drying shrinkage, importance weight of 5;

✓ Carbon dioxide emission, importance weight of 3;

✓ Cost, importance weight of 5.

In addition to the reference binder employed by the MoDOT (75% Type I cement + 25% Class C fly ash), two ternary binders were optimized for the concrete investigation: (1) a ternary blend of 35% class C fly ash + 15% ground granulated blast furnace slag; and (2) a ternary blend of 35% class C fly ash + 15% glass powder.

The investigation of concrete performance included the evaluation of fresh properties, mechanical properties, and shrinkage of several concrete mixtures made with different fine and

9

coarse RCA contents, as summarized in Table 3. The following scenarios were considered for concrete production:

✓   Sustainable concrete for single layer rigid pavement;

✓   Sustainable concrete for two-lift concrete pavement (2LCP).

The 2LCP systems are composed of two wet-on-wet layers of concrete. Given the coverage provided by the high-quality top layer, a mixture incorporating high-volume recycled materials can be incorporated for the bottom lift in the 2LCP systems.

The optimized mixtures developed 28-d compressive strengths ranging from 4,600 to 7,100 psi (31.7 to 49.0 MPa) and 91-d compressive strengths of 5,900 to 8,600 psi (40.7 to 59.3 MPa). The investigated mixtures had flexural strengths higher than 600 psi (4.15 MPa) at 28 d, except for the mixture made with 70% of coarse RCA and 15% of fine RCA (70C15F).

The MOE values ranged from 4.1 to 6.2 ksi (28.3 to 42.7 GPa) and 4.7 to 6.7 ksi (32.4 to 46.2 GPa) at 28 and 56 d, respectively. Increasing the coarse and fine RCA contents to values higher than 60% and 30%, respectively, reduced the MOE significantly (up to 30%). However, the use of proper mixture proportioning and binder composition made it possible to maintain the minimum desired MOE.

Using the optimized binder composition incorporating 35% Class C fly ash and 15% slag cement reduced the 150-d drying shrinkage of mixtures cast with 50% coarse RCA and 15% fine RCA to less than 350 to 500 µε. However, the increase in fine RCA content from 15% to 40% resulted in greater shrinkage values of up to 650 µε. Decreasing the w/cm from 0.40 to 0.37 was effective in reducing shrinkage of mixtures with 50% RCA content (450 µε at 150 days). All mixtures proportioned with the optimized binder made with 35% Class C fly ash and 15% slag cement and w/cm of 0.37 and 0.40 developed adequate electrical resistivity, with values ranging

from 27 to 50 kΩ·cm at 90 d, compared to 19 kΩ·cm for the reference PCCP mixture. Table 4 offers a summary of key mechanical properties obtained from testing of all the investigated concrete mixtures.

Table 3 - Test matrix for concrete optimization

Mixture No.		Concrete type		C-RCA (%)	F-RCA (%)	w/cm	Binder type
1	MoDOT PCCP			0	0	0.40	25% FA-C
2	Opt. Binder			0	0	0.40	35%FA-C+15%SL
3	30C-GP-37		Top layer	30	0	0.37	35%FA-C+15%GP
4	30C-37			30	0	0.37	
5	30C			30	0	0.40	
6	30C15F-37			30	15	0.37	
7	30C15F			30	15	0.40	
8	40C15F	Single layer		40	15	0.40	
9	50C-37			50	0	0.37	
10	50C			50	0	0.40	35%FA-C+15%SL
11	50C15F-37			50	15	037	
12	50C15F			50	15	0.40	
13	50C30F			50	30	0.40	
14	50C40F			50	40	0.40	
15	60C30F	Bottom layer		60	30	0.40	
16	70C-37			70	0	0.37	
17	70C			70	0	0.40	
18	70C15F			70	15	0.40	
19	70C30F			70	30	0.40	

Table 4 - Mechanical properties of investigated mixtures

Mixture		Compressive strength (psi)			Splitting tensile strength (psi)		Flexural strength (psi)		Modulus of elasticity (ksi)	
		1 d	28 d	91 d	28 d	56 d	28 d	56 d	28 d	56 d
1	MoDOT	2,180	5,590	6,750	460	500	710	700	6,200	5,915
2	Opt. Binder	1,240	6,020	7,330	400	470	650	770	5,850	6,415
3	30C-GP-37	950	7,110	8,850	390	440	750	920	6,225	6,725
4	30C-37	1,820	6,380	8,630	490	490	810	780	6,125	6,200
5	30C	1,240	5,800	6,600	370	500	700	720	5,400	5,570
6	30C15F-37	1,670	7,110	8,130	440	460	750	760	5,950	6,750
7	30C15F	1,020	5,370	6,650	390	490	660	630	5,085	4,925
8	40C15F	950	4,570	5,880	340	450	610	710	4,425	4,765
9	50C-37	1,090	6,820	7,910	430	420	730	750	5,500	5,850
10	50C	1,240	5,880	6,960	420	370	720	770	5,200	5,415
11	50C15F-37	870	6,020	7,110	410	420	720	740	5,250	5,450
12	50C15F	1,160	5,590	5,950	390	400	600	730	4,900	5,165
13	50C30F	1,020	4,640	6,310	450	420	630	720	4,115	4,915
14	50C40F	1,020	4,560	6,020	320	370	680	640	4,115	4,785
15	60C30F	1,160	5,380	6,240	350	340	680	610	4,550	4,915
16	70C-37	870	6,750	7,690	440	440	730	760	5,475	5,500
17	70C	1,090	5,300	6,460	310	380	640	690	4,767	4,900
18	70C15F	960	5,080	6,460	420	390	550	580	4,200	4,735
19	70C30F	1,240	5,370	6,240	420	420	690	730	4,615	4,950

The test results were analyzed, and selected concrete mixtures were further investigated for durability, including resistance to freezing and thawing, de-icing salt scaling, abrasion resistance, and sorptivity. Table 5 summarizes the durability results of concrete mixtures that exhibited satisfactory mechanical properties and shrinkage characteristics.

Table 5 - Durability of investigated mixtures

Mixture		Frost durability factor (%) ASTM C666, A	Scaling resistance rating ASTM C672	Mass loss due to scaling (g/m^2)	Abrasion mass loss (g)	Initial sorptivity $(mm/s^{0.5})$	Secondary sorptivity $(mm/s^{0.5})$
1	MoDOT	95.6	1	100	1.2	2.23 E-6	8.9 E-7
2	Opt. binder	92.5	3	735	1.2	1.49 E-6	5.5 E-7
3	30C-GP-37	88.8	4	1,230	0.4	0.95E -6	3.5 E-7
4	30C-37	97.1	3	640	0.8	1.23 E-6	5.1 E-7
5	30C	90.5	3	870	1.3	1.89 E-6	6.0 E-7
6	30C15F-37	96.0	3	640	0.7	0.86 E-6	3.7 E-7
7	30C15F	94.5	3	1,190	1.1	1.59 E-6	6.2 E-7
8	50C-37	92.2	3	700	0.5	1.23 E-6	5.0 E-7
9	50C15F-37	96.0	3	800	0.7	1.13 E-6	4.9 E-7
10	70C-37	96.0	2	450	0.7	1.29 E-6	5.3 E-7

Increasing the RCA content did not have a significant effect on abrasion resistance. The investigated mixtures exhibited similar resistance to abrasion damage with mass loss limited to 0.07 ounce (2.0 g). The investigated mixtures had durability factors higher than 89%, regardless of the RCA content, thus indicating excellent frost durability. The mixtures made RCA exhibited considerable higher de-icing salt mass loss than that of the reference MoDOT mixture. The mass loss after 50 cycles of freezing and thawing of RCA mixtures was limited to 25.7 oz/yd^2 (870 g/m^2), which is considered adequate; this is in exception of two mixtures in Table 5 that exceeded the upper limit of (29.5 oz/yd^2) [1000 g/m^2]. All of the investigated mixtures had comparable CTE values ranging from 4.8 to 5.2 10^{-6} in./in./°F (8.6 to 9.4 μm/m/°C).

3.2 RECOMMENDED MIXTURES FROM PHASE I

Concrete mixtures incorporating high volume recycled aggregate and SCMs can present a viable choice for sustainable pavement construction. The following mixtures exhibited satisfactory performance for the construction of the single layer and two-lift pavement systems:

Single layer pavement:

4. Reference concrete cast without any RCA proportioned with 0.40 w/cm and 25% Class C fly ash replacement (this corresponds to the MoDOT PCCP reference concrete).

5. Concrete incorporating 15% slag cement and 35% Class C fly ash replacements proportioned with 0.40 w/cm without any RCA (optimized binder).

6. Concrete made with 15% slag cement and 35% Class C fly ash replacements proportioned with 0.40 w/cm and 30% coarse RCA (30C).

7. Concrete incorporating 15% slag cement and 35% Class C fly ash replacements proportioned with 0.37 w/cm and 50% coarse RCA (50C-37).

Table 6 offers a summary of the properties of the proposed mixtures for use in single layer pavement.

Table 6 - Performance of the proposed mixtures for use in single layer pavement

Property	MoDOT PCCP	Opt. binder	30C	50C-37
28-d Compressive strength (psi)	5,590	6,020	5,800	6,820
91-d Compressive strength (psi)	6,750	7,330	6,600	7,910
56-d Modulus of elasticity (ksi)	5,920	6,420	5,570	5,850
56-d Flexural strength (psi)	700	770	720	750
90-d Shrinkage ($\mu\varepsilon$)	430	340	450	420
Frost durability factor (%)	96	93	91	92
De-icing salt scaling rating	1	3	3	3
De-icing salt mass loss (g/m^2)	100	735	870	700
(oz/yd^2)	2.95	21.7	25.7	20.6

Two-lift concrete pavement:

8. Reference concrete mixture cast without any RCA proportioned with 0.40 w/cm and 25% Class C fly ash replacement for the top layer (MoDOT PCCP reference concrete).

9. Concrete incorporating 15% slag cement and 35% Class C fly ash replacements, 0.40 w/cm, without any RCA for the top layer (optimized binder).

10. Concrete incorporating 15% slag cement and 35% Class C fly ash replacements, 0.40 w/cm, and 30% coarse RCA for top layer (30C).

11. Concrete incorporating 15% slag cement and 35% Class C fly ash replacements, 0.37 w/cm, 50% coarse RCA, and 15% fine RCA for bottom layer (50C15F-37).

12. Concrete incorporating 15% slag cement and 35% Class C fly ash replacements, 0.37 w/cm, and 70% coarse RCA for bottom layer (70C-37).

Table 7 offers a summary of the properties of the proposed mixtures for use in 2LCP.

Table 7 - Performance of the proposed mixtures for use in 2LCP

Application	Top layer			Bottom layer	
Property	MoDOT PCCP	Opt. Binder	30C	50C15F-37	70C-37
28-d Compressive strength (psi)	5,590	6,020	5,800	6,020	6,750
91-d Compressive strength (psi)	6,750	7,330	6,600	7,110	7,690
56-d Modulus of elasticity (ksi)	5,920	6,420	5,570	5,450	5,500
56-d Flexural strength (psi)	700	770	720	740	760
90-d Shrinkage (με)	430	340	450	490	450
Durability factor (%)	96	93	91	96	96
De-icing salt scaling rating	1	3	3	3	2
De-icing salt mass loss (g/m²)	100	735	870	800	450
(oz/yd²)	2.95	21.7	25.7	23.6	13.3

4. INSTRUMENTATION

The details of sensors and data acquisition systems required were finalized in collaboration with MoDOT engineers. The required sensors and data acquisition systems were properly designed and procured. Two data acquisition systems were prepared to monitor changes in deformation, temperature, and RH in concrete elements as a function of time. Table 8 summarizes the list of instrumentation used for the data acquisition system. The following describes the instrumentation for slab and beam specimens that can be used for field implementation of sustainable concrete made with RCA.

Table 8 - Equipment required for instrumentation

Item	Number
Data acquisition system	2
Solar panel	2
Concrete strain gauge	72
Relative humidity sensor	36
Thermocouple	4 rolls
Wire	16 rolls
Modem	2

The embedment type of strain gauges (KM-120-120-H2-11, manufactured by KYOWA) was considered to monitor concrete shrinkage, as shown in Figure 1. The sensor has an outer body of 120 mm (4.7 in.) sensing grid with an effective gauge length of 75 mm (3.0 in.). The gauge is waterproof and is designed to be placed in fresh concrete to directly measure shrinkage deformation associated with the concrete mixture.

Figure 1 - Embedded strain gauge for monitoring shrinkage deformation

The selected thermocouple system (UX-08542-24, manufactured by Coleparmer) was a Type T 20 gauge wire. These thermocouples consist of copper and constantan wires and are functional between -250 to 250° C (-418 to 482 °F). The ends of the solid thermocouple wires were twisted and then soldered to ensure an adequate electrical connection, as shown in Figure 2.

Figure 2 - Thermocouple used for concrete temperature measurement

The small (6 × 20 mm [0.24 × 0.79 in.]) capacitive RH sensor (HIH-4030, manufactured by Sparkfun) was considered to measure the RH inside the concrete. The accuracy of the sensors reported by the manufacturer is ± 2% RH between 10% and 90% RH, and ranges up to ± 4% at 100% RH. In order to embed the RH sensor in concrete, the RH sensor is placed inside a PVC tube, and the end of the tube is covered by Gore-Tex to allow moisture transmission, while preventing the penetration of liquid water and solid particles that may lead to an error in measurement. Figure 3 shows the encapsulated RH sensor before installation in concrete.

Figure 3 - Encapsulated relative humidity sensor before embedment in concrete

Figure 4 shows the proposed instrumentation layout, including embedded concrete strain gauges, RH sensors, and thermocouples for monitoring shrinkage of concrete used for pavement construction. Sensors were placed at different locations/heights to monitor concrete shrinkage at various depths along the thickness of concrete slabs.

(a)   (b)
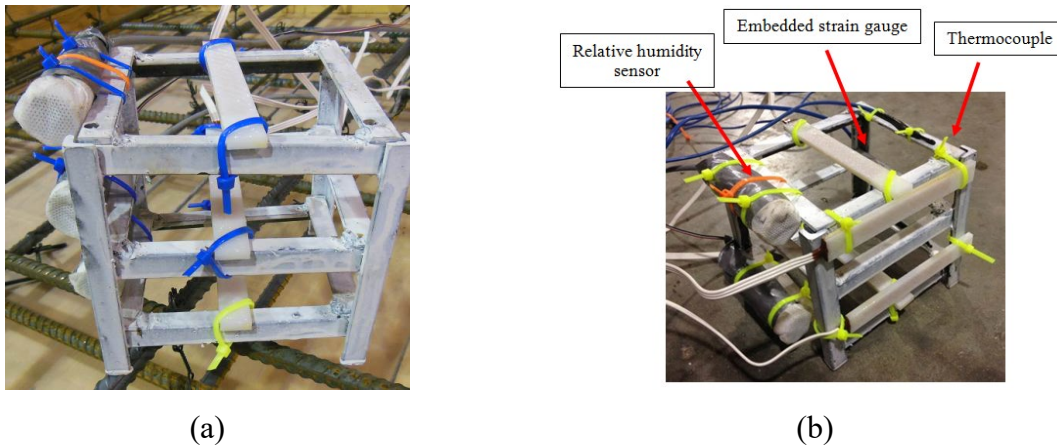
Figure 4 - Instrumentation layouts for (a) Layout A: 3 embedded strain gauges in longitudinal direction, 3 thermocouples and RH sensors, and (b) Layout B: 4 embedded strain gauges (2 longitudinal and 2 transverse directions), 2 thermocouples and RH sensors

Both strain and temperature data can be recorded using Campbell Scientific Data acquisition hardware and software systems. Lead wires from the strain gauges can be routed through either an AM416 or an AM16-32 multiplexer, using a separate completion module for each gauge on the multiplexer, or using a single completion module for all the gauges that can be

positioned between the multiplexer and the datalogger, as shown in Figure 5. The system is

powered by a 12 V battery for which the charge is maintained using a solar panel.
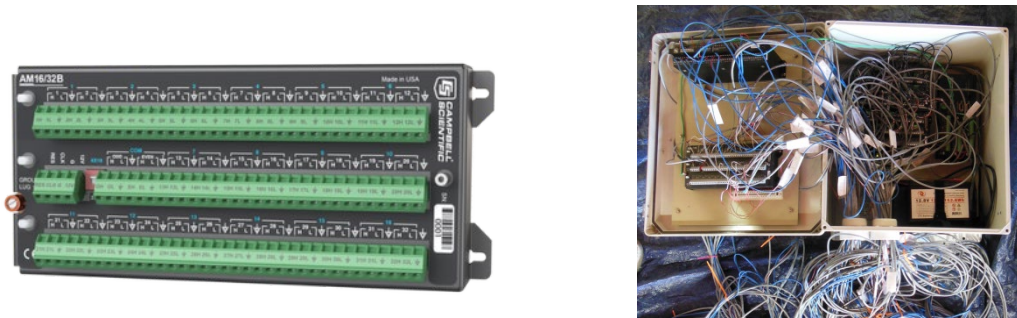
Figure 5 - Data acquisition system used for data collection

5. LIFE CYCLE COST ANALYSIS

One of the main advantages of using RCA in concrete production is the reduced need of using non-renewable natural resources, such as natural aggregates. This can also reduce the amount of construction and demolition wastes dumped into landfills. If recycling (concrete into aggregate) is performed in place, there will be savings in hauling distance of the aggregate from quarry to the job site as well. This will reduce transportation emissions, cost, and time.

As for environmental impact, using high-volume SCMs can be an effective means of reducing the carbon footprint of the concrete. In addition, using proper amounts and types of SCMs can lead to improved mechanical properties and durability of concrete, which in turn enhances the service life and compensates for the potential negative impacts associated with the use of RCA. The estimated material unit costs and service life improvement rates obtained for optimized mixtures are shown in Table 9. They are the best-guess values based on a combination of compressive strength, flexural strength, MOE, and drying shrinkage laboratory results. These values could be further evaluated once field implementation data become available.

Given the potential for on-site recycling, high-volume recycled materials tested in this project can decrease construction time, labor, and equipment needed on construction sites. The following highlights potential improvements of the high-volume recycled materials compared with typical practice using the reference mixture.

✓ Decrease in construction time, labor, and equipment needed on construction sites;

✓ Reduced costs and emissions related to cement consumption;

✓ Reduced need for landfills and use natural resources by using recycled aggregate in new concrete production;

✓ Potentials for reducing the hauling distance for aggregate;

✓   Improved quality and service life can be expected.

Table 9 - Estimated material unit prices and service life improvement rates

Mixture	Unit price ($/CY)	Relative improvement compare to reference mixture (%)
MoDOT reference mixture	45.2	-
Optimal binder	44	10.3
30C-37	44.5	3.0
50C-37	43.3	-3.1
50C15F-37	43.1	-8.1
60C30F	43.7	-33.2
70C-37	43.8	-5.1

Deterministic pavement life cycle cost analysis (LCCA) examples were built for the MoDOT reference mixture and six different high-volume recycled materials mixtures selected in Phase I using the improvement rate approach. The LCCA for the case study presented here was conducted in collaboration with Professor Kaan Ozbay and his team at New York University as part of a collaboration of the RE-CAST Tier-1 University Transportation Center. Since the proposed high-volume recycled materials studied here are supposed to be used as construction materials, the maintenance costs are assumed to be the same and are neglected in this case study. According to a survey conducted by the RE-CAST team, the average construction unit cost in Missouri in 2016 was \$53/yd^2 for the construction of a 9-in. (229-mm) thick concrete pavement, which is used for the reference concrete. Also, a 0.25-in. (6-mm) diamond grinding and full-depth repair (1.5% slab replacement is required in the travel lane) is assumed to happen after 25 years for the MoDOT reference mixture. The same treatment was applied for this project's concrete mixture based on its estimated rehabilitation schedule. In addition, the following assumptions were

made for the concrete with improved workability in terms of labor costs and construction time savings: 1) the labor costs for the placement and consolidation will be reduced by 20%; 2) the patching labor costs will be reduced by 30%; and 3) the construction time for rehabilitation will be reduced by 10%.

The case study project chosen for this research objective is a highway section on US 50 in Osage County, Missouri. This paving project is approximately 6.634 miles (10.68 km) in length and starts at logmile 152.6 and ends at logmile 159.234. It has two 13-ft (3.9-m) wide lanes in each direction with asphalt shoulders. The Average Daily Traffic (ADT) of this section is 12,420 vehicles, and 8.5% of the total vehicles are trucks. The traffic growth rate is assumed to be 2.2%. Table 10 lists the detail input information for this pavement example, and Table 11 lists the deterministic output results. Note that for Table 10 and Table 11, a reference concrete mixture used by MoDOT and the optimal binder of Phase I were used to establish the workflow.

Computing the construction cost of a pavement alternative involves not only the material quantity calculations, but also the other direct and indirect costs associated with the pavement alternative being considered (CDOT 2016). In the proposed pavement LCCA approach, the cost of preliminary engineering, miscellaneous and mobilization are included in both initial construction and rehabilitation cost. The estimated percentage of such costs are based on average values retrieved from MoDOT's pavement design and type selection process report (MODOT 2004). When using the optimal binder of the new material in this project, the final deterministic pavement LCCA results given in Table 11 show that the application of the new material will save 17.6% of agency costs, 12.1% of user cost, 12.1% of social cost, and 17.5% of total life cycle cost. In this case study, the user costs are only calculated for stopped queues under work zone conditions.

Table 10 - LCCA example work flow – inputs

I. Analysis options	Alt 1: MoDOT reference concrete	Alt 2: Project 2-A opt. binder
1. Service life (year)	25	28
2. Analysis period (year)	45	45
3. Discount rate (%)	3.0%	3.0%
4. Material unit price ($/CY)	45.2	44.0
5. Construction unit cost ($/SY)	53.00	48.69
II. Traffic data		
Average daily traffic (veh/day):	12,420	
Trucks as percentage of ADT (%):	8.50%	
Annual growth rate of traffic (%):	2.2%	
Lanes opened under normal condition:	Inbound (2), outbound (2)	
Value of time ($/hr):	11.58 (Passenger car), 20.43 (Truck)	
III. Work zone input		
Maintenance schedule:	Maintenance schedule/cost are assumed to be the same for both alternatives and are neglected in this study	
Rehabilitation/replacement schedule:	Time to first rehabilitation: 25 years (rehabilitation extended service life: 20 years)	Time to first rehabilitation: 28 years (rehabilitation extended service life: 20 years)
Rehabilitation duration (days):	30	27
# lanes opened during maintenance/rehab:	1 lane	1 lane
Free flow speed (mph):	70	70
Work zone speed-maintenance (mph):	50	50
Work zone speed-rehabilitation (mph):	30	30

Table 11 - LCCA example work flow – deterministic outputs

I. Agency cost ($)	Alt 1: MoDOT Reference Concrete	Alt 2: Project 2-A Opt. Binder
Initial construction cost ($):	8,187,943	6,904,562
Maintenance cost ($):	Maintenance cost is assumed to be the same for both alternatives and are neglected in this study	
Rehabilitation cost:		
(A) Slab replacement ($):	188,484	172,489
(B) Treatment - diamond grinding ($)	174,952	160,106
(C) Miscelleneous & mobilization ($)	52,445	47,995
(D) Preliminary engineering ($)	43,704	39,996
Total rehabilitation cost (s):	459,585	420,585
Salvage value ($):	0	-195,625
Total agency cost ($):	$8,647,528	$7,129,522
II. User cost ($)		
Traffic delay cost ($):	$0	$0
Vehicle operation cost ($):	$0	$0
Crash risk cost ($):	$255,618	$224,737
Total user cost ($):	$255,618	$224,737
III. Social cost ($)		
Air Pollution cost ($):	$74,260	$65,289
Total Social cost ($):	$74,260	$65,289
IV. Total life cycle cost	$8,798,473	$7,262,232
Alt 2: Project 2-A optimal binder benefit	Total life cycle cost: -17.5% Agency cost: -17.6%, user cost: -12.1%, social cost: -12.1% (User cost factor: 0.3, social cost factor: 1.0)	

Since the traffic volume on the study highway segment will not exceed the highway capacity under work zone conditions, traffic delay costs and vehicle operation costs are taken as zero. Furthermore, based on the information provided in Table 10, the research team applied LCCA to multiple mixtures selected in Phase I. Their relative differences in total life cycle cost compare with that of MoDOT reference mixture, as shown in Figure 6. Most of the sustainable mixtures made with RCA provided 15% to 18% cost savings in terms of the total life cycle cost.
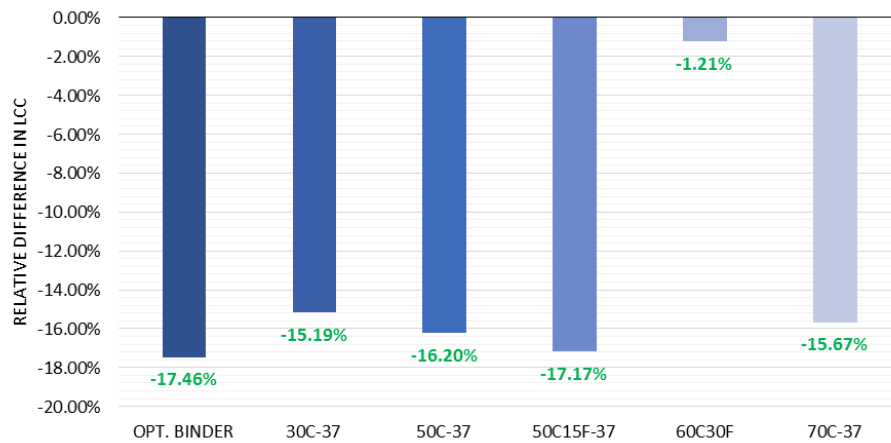

Figure 6 - Relative difference in LCCA of multiple mixtures

6. ARTIFICIAL INTELLIGENCE FOR INVESTIGATING EFFECT OF RCA ON CONCRETE PROPERTIES

As stated earlier, the mechanical properties and durability of concrete made with RCA can be significantly impacted when using RCA materials of inferior quality compared to that of the virgin aggregate. The MOE is one of the characteristics of concrete that is highly sensitive to the incorporation and quality of RCA. The availability of residual mortar in RCA particles can reduce the overall stiffness and restraining capacity of the coarse aggregate skeleton and increase the absolute volume of mortar in the hardened state. This can reduce the rigidity of the concrete, resulting in a lower MOE compared to the corresponding mixtures prepared without any RCA. Moreover, the presence of micro-cracks in the residual mortar, old virgin aggregate, and the old interfacial transition zone (ITZ) between these two phases (anticipated due to the crushing procedure), can significantly affect the MOE.

Considering the fact that MOE is one of the main features to affect the design and performance of rigid pavements, it was decided in this project to develop a model to estimate the variations in MOE of concrete. The model development involved three main phases. The first phase included the development and screening of a database of published literature on the MOE of concrete made with coarse RCA. The second phase was to generate laboratory data to validate the model. The third phase involved testing the model based on artificial neural networks (ANN). These steps are further elaborated in what follows.

6.1 DEVELOPMENT AND ANALYSIS OF THE DATABASE

The database that was established to correlate the MOE of concrete with the key parameters affecting it consisted of 484 data series obtained from 52 published articles. Details regarding the

model development are available in Sadati et al. (2019). The 28-day compressive strength of the investigated concrete mixtures ranged from a minimum of 2,180 psi (15 MPa) to approximately 15,900 psi (110 MPa). The minimum and the maximum MOE values were 1,600 and 8,000 ksi (11 and 55 GPa), respectively. Each dataset included a summary of the concrete mixture design, virgin aggregate content and properties, and coarse RCA content and characteristics. The investigated input factors are elaborated below.

Binder: binder content (kg/m^3) and binder type, which was considered as a categorical factor of 1 or 2. An input value of 1 was attributed to the concrete with plain portland cement (OPC), while binder type 2 was used for concrete mixtures with SCM.

Water: water-to-binder ratio (w/b), water-to-cement ratio (w/c), and water content (kg/m^3).

Fine aggregate: fine aggregate content (kg/m^3).

Virgin coarse aggregate: virgin coarse aggregate content (kg/m^3), virgin coarse aggregate water absorption (%), virgin coarse aggregate oven-dry specific gravity, and virgin coarse aggregate Los Angeles (LA) abrasion value (%).

Coarse RCA: coarse RCA (C-RCA) content (kg/m^3), coarse RCA water absorption (%), coarse RCA oven-dry specific gravity, coarse RCA LA abrasion value (%), and coarse RCA replacement ratio (% mass).

Total coarse aggregate: total coarse aggregate content (kg/m^3), combined coarse aggregate water absorption (%), combined coarse aggregate oven-dry specific gravity, and combined coarse aggregate LA abrasion value (%). The combined coarse aggregate properties were calculated as a linear combination of the properties and relative mass of the blend constituents, as proposed by Omary et al. (2016). Equations (1-3) were used to determine the oven-dry specific gravity, water

absorption, and mass loss due to LA abrasion, respectively, of a given combination of coarse aggregate, respectively, as suggested by Omary et al. (2016).

$$Coarse_{SG} = [(Mass_{RCA} \times RCA_{SG}) + (Mass_{NC} \times NC_{SG})]/(Mass_{RCA} + Mass_{NC}) \qquad (1)$$

$$Coarse_{Abs} = [(Mass_{RCA} \times RCA_{Abs}) + (Mass_{NC} \times NC_{Abs})]/(Mass_{RCA} + Mass_{NC}) \qquad (2)$$

$$Coarse_{LA} = [(Mass_{RCA} \times RCA_{LA}) + (Mass_{NC} \times NC_{LA})]/(Mass_{RCA} + Mass_{NC}) \qquad (3)$$

where $Mass_{RCA}$ is the RCA content (kg/m^3), $Mass_{NC}$ is the virgin coarse aggregate content (kg/m^3), RCA_{SG} is the oven-dry specific gravity of RCA, NC_{SG} is the oven-dry specific gravity of the virgin coarse aggregate, RCA_{Abs} is the water absorption of the RCA (%), NC_{Abs} is the virgin coarse aggregate absorption rate (%), RCA_{LA} is the mass loss due to LA abrasion of RCA (%), NC_{LA} is the mass loss due to LA abrasion of the virgin coarse aggregate (%), and $Coarse_{SG}$, $Coarse_{Abs}$, and $Coarse_{LA}$ are the oven-dry specific gravity, water absorption rate (%), and LA abrasion (%) of the coarse aggregate combination, respectively.

Table 12 offers a summary of the input features along with the corresponding minimum and maximum values. Four different scenarios of input factors were explored to ensure the most generalized and robust predictions with the lowest chance of overfitting the data. Development of a comprehensive model requires the employment of user-friendly, yet representative indices to depict the RCA quality. One should note that the heterogeneous nature of RCA makes it impossible to define representative indices at the micro level. Therefore, the considered RCA properties included water absorption, specific gravity, and mass loss due to LA abrasion, which are also employed by the standards, recommendations, and guidelines to define RCA quality (Khayat and Sadati 2016). The investigated input scenarios are elaborated below and summarized in Table 12.

Table 12 - ANN model input and output parameters for database and laboratory mixtures

Parameter		Database				Laboratory				Scenario			
		Min.	Max.	Avg.	Std.*	Min.	Max.	Avg.	Std.*	I	II	III	IV
Input Parameters	1 Binder content (kg/m³)	210	609	375.2	65.5	317	323	322	2	*	*	*	*
	2 Binder type	1: OPC	2: SCM	-	-	2	2	-	-	*	*	*	*
	3 Virgin coarse content (kg/m³)	0	1950	558.0	444.0	0	1136	632	310	*	*	*	*
	4 Coarse RCA content (kg/m³)	0	1800	501.9	435.0	0	964	410	260	*	*	*	*
	5 water/binder (w/b)	0.25	0.87	0.48	0.11	0.37	0.45	0.40	0.02	*	*	*	*
	6 water/cement (w/c)	0.29	1.22	0.52	0.14	0.53	0.80	0.63	0.11	*	*	*	*
	7 Fine aggregate content (kg/m³)	465	1301	726	126	772	795	785	7	*	*	*	*
	8 Coarse aggregate absorption (%)	0.20	6.10	1.26	0.80	0.50	0.98	0.80	0.10	*	*	*	*
	9 C-RCA absorption (%)	1.93	18.91	5.39	2.41	4.20	7.58	5.40	1.17	*	*	*	*
	10 Coarse specific gravity, OD (kg/m³)	2483	2880	2607	82	2640	2730	2719	23	*	*	*	*
	11 C-RCA specific gravity, OD (kg/m³)	1800	2602	2313	125	2170	2380	2297	73	*	*	*	*
	12 Coarse aggregate NMAS (mm)	8	32	20.1	4.0	19	19	19	0	*	*	*	*
	13 Coarse RCA NMAS (mm)	8	32	19.0	4.9	13	19	18	2	*	*	*	*
	14 Coarse aggregate LA abrasion (%)	14	43	20.8	6.0	24	43	29.3	5.1			*	*
	15 C-RCA LA abrasion (%)	13.7	81.7	33.8	8.8	33	53	39.3	6.2			*	*
	16 water content (kg/m³)	108	234	175	30	120	143	128	7		*		*
	17 Total coarse aggregate content (kg/m³)	640	1950	1060	143	907	1136	1042	53		*		*
	18 Coarse combination absorption (%)	0	16	3.2	2.0	0.50	7.13	2.70	1.40		*		*
	19 Coarse combination specific gravity, OD	1800	2880	2467	144	2210	2730	2543	123		*		*
	20 Coarse combination LA abrasion (%)	13.7	51.5	27	8	24	53	33.5	5.5				*
	21 Coarse RCA replacement ratio	0	1	0.5	0.4	0	1	0.4	0.3		*		*
Output	Relative MOE (R_{MOE})	0.44	1.37	0.89	0.12	0.67	1.05	0.89	0.09				

*Standard deviation
1 kg/m³ = 1.686 lb/yd³

Scenario I: The input factors included 13 independent properties summarizing the key mixture design details, virgin aggregate properties, and RCA characteristics. The aggregate-related properties included the aggregate content (kg/m^3), oven-dry specific gravity, and water absorption (%) for both the virgin and RCA materials. The LA abrasion value was not included in the first scenario, since not all of the investigated sources from the literature reported these values for RCA.

Scenario II: A total number of 18 input factors were investigated for the second scenario. The input parameters included the 13 independent properties (elaborated on in scenario I) and an additional set of five dependent parameters. The aggregate-related properties considered in the second scenario included the aggregate content (kg/m^3), oven-dry specific gravity, and water absorption (%) for both the virgin and RCA materials. Again, the LA abrasion of the coarse virgin aggregate and RCA were not included in the analysis. The additional dependent variables were the total water content in the mixture, total coarse aggregate content (kg/m^3), RCA replacement ratio (% mass) of coarse aggregate, combined coarse aggregate oven-dry specific gravity, and combined coarse aggregate water absorption (%); the last two values were calculated using Equations 1 and 2, respectively.

Scenario III: A total number of 15 independent input parameters were considered for the third scenario. The 13 factors elaborated on scenario I were incorporated along with the LA abrasion values of the virgin coarse aggregate and the RCA materials. As stated earlier, not all of the investigated references reported the LA values of the aggregate. Therefore, based on the data reported in the literature, in addition to a laboratory investigation that was undertaken here, correlations were established between the LA abrasion and the water absorption and specific gravity of the RCA as suggested by González-Taboada et al. (2016). Figure 7 presents the correlations between the LA abrasion and the water absorption developed by González-Taboada

et al. (2016) and further updated by the authors obtained from over 100 different RCA types. A strong linear correlation was observed, with a R^2 value of 0.75 for the relationship between the LA abrasion and the water absorption. The correlation established in Figure 7 was employed to estimate the LA abrasion for concrete mixtures where actual values were missing data points of the database.
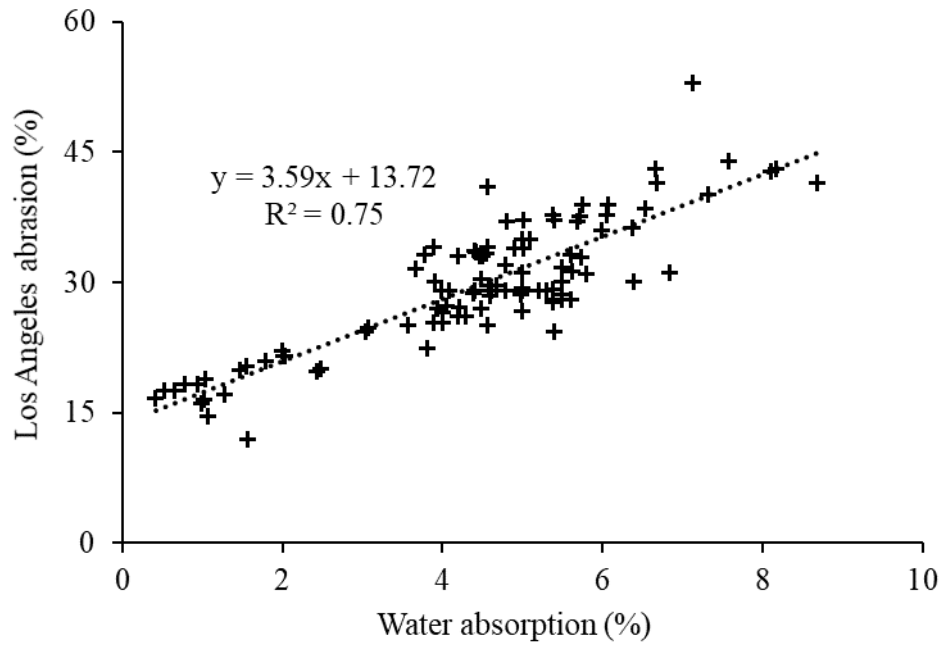

Figure 7 - Correlation between LA abrasion and water absorption

Scenario IV: A total number of 21 input parameters were included in this scenario. The aggregate-related properties considered in this scenario included the aggregate content (kg/m³), oven-dry specific gravity, water absorption (%), and LA abrasion (%) for both the virgin and RCA materials. The additional dependent variables were the water content in the mixture, total coarse aggregate content (kg/m³), RCA replacement ratio (% mass), combined coarse aggregate water absorption (%), combined coarse aggregate oven-dry specific gravity, and combined coarse aggregate LA abrasion (%) calculated using Equations (1), (2), and (3), respectively.

Output: the output of the study was the relative variation in MOE, defined in Equation (4).

$$R_{MOE} = \frac{MOE \ of \ concrete \ made \ with \ RCA}{MOE \ of \ corresponding \ reference \ concrete \ made \ without \ RCA} \tag{4}$$

A relative performance value of 1.0 was considered for the control mixture (proportioned without any RCA) of each study reported in the database. Considering the relative MOE (R_{MOE}) as the means of comparison reduces the uncertainties related to non-uniform experimental conditions, e.g. air content in the hardened state, specimen size, test device, loading rate, and test protocol, etc., typical of database analysis. This way, one can assume that there are no significant correlations between the aforementioned factors and the relative performance of the mixtures.

6.2 LABORATORY DATA

Material properties. In total, 43 different concrete mixtures were produced in the laboratory. Type I/II portland cement, Class C fly ash (FA-C), and ground granulated blast furnace slag (GGBS) were used as binder materials. The mixtures were proportioned with either binary or ternary cement. The binary cement was composed of 75% (by mass) OPC and 25% FA-C. The ternary system incorporated 35% FA-C and 15% GGBS. The binary cement was adopted from the concrete mixture design employed by the Missouri Department of Transportation (MoDOT) for rigid pavement construction Khayat and Sadati (2016). The ternary system was optimized based on the mechanical properties and shrinkage of concrete equivalent mortar prepared with w/cm of 0.40, developed by Khayat and Sadati (2016). Three different water-to-cementitious materials ratios (w/cm) of 0.37, 0.40, and 0.45 were considered during the design of the concrete mixtures. Coarse RCA procured from six different sources, including five recycling centers and one

laboratory produced RCA, were considered. A siliceous river sand was incorporated as fine aggregate. The aggregate properties were introduced earlier in Table 1. An air entraining agent was used to secure 6% ± 1% air in fresh concrete. A water reducing admixture was incorporated to adjust the initial slump values.

   Concrete preparation and testing. A drum mixer with 0.26 gallon (110-L) capacity was used for concrete mixing. Slump and air content in the fresh state were determined according to ASTM C143 and ASTM C231, respectively. Cylindrical specimens measuring 3.9 × 7.9 in. (100 × 200 mm) were employed to determine the compressive strength and MOE according to ASTM C39 and ASTM C469, respectively. A vibrating table was employed to secure proper consolidation of the concrete. Extracted samples were then covered with wet burlap and plastic sheets up to 24 hours after casting. The specimens were cured in lime-saturated water at 70 ± 3 ºF (21 ± 2 ºC) up to the testing time at 28 days.

6.3 MODEL DEVELOPMENT

   Inspired by the biological nervous system, the ANNs are information analysis paradigms that are widely used as computational tools. Concretely, an ANN is a universal function approximator that builds the mapping between an input and an output space. Modeling using ANN involves five main steps: (1) representing the problem and acquiring the data; (2) defining the architecture; (3) determining the learning process; (4) training the network; and (5) testing the developed network to ensure robustness and generalization (Duan et al., 2017). Neural networks are composed of a large number of interconnected artificial processing units, known as neurons. Usually, these neurons are arranged in layers (input, hidden, and output), which in turn are fully connected; the number of neurons per layer defines the ANN architecture. Each neuron typically consists of five different parts: inputs, weights, transfer function, activation function, and output,

as illustrated in Figure 8. The transfer function used in this study is the weighted sum presented in

Equation (5):

$$net_j = \mathbf{w}^T \mathbf{x} = \sum_{i=0}^{n} w_{ij} x_i \tag{5}$$

where $\mathbf{x}$ represents the input vector applied to a given neuron associated with weight vector $\mathbf{w}$; thus, net_j is the weighted sum of the jth neuron based on its weights and input values from n neurons of the preceding layer, w_{ij} is the weight factor between the jth neuron and the ith neuron of the preceding layer, whose output is x_i, and $b = w_{0j} x_0$ is the bias ($x_0 = 1$).
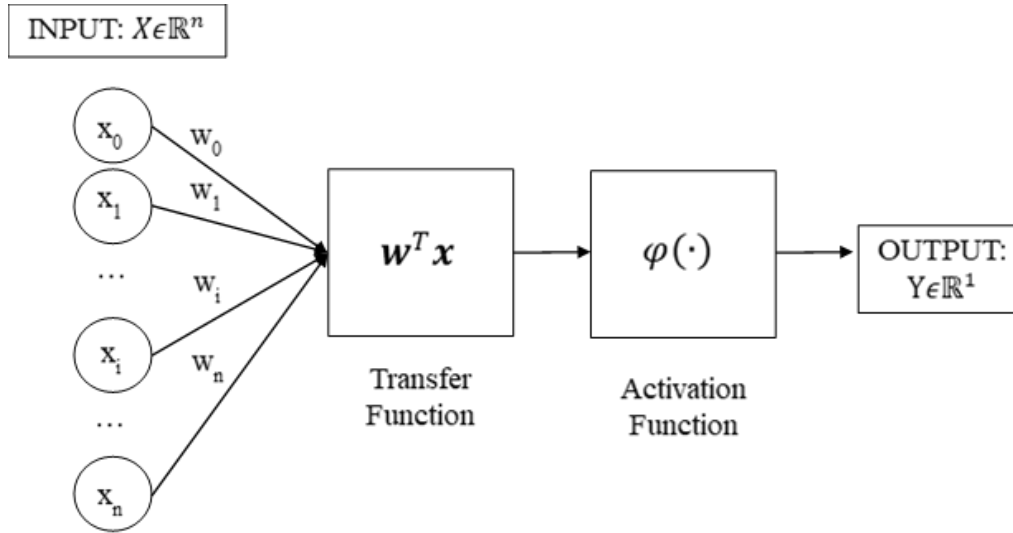

Figure 8 - Schematic structure of a simple neuron model

The activation function $\varphi(net_j)$ translates the *net* value to the neuron output. A variety of activation functions were presented in the literature, such as linear, sigmoid, and hyperbolic tangent sigmoid, etc. In this study, the activation functions of the output and hidden neurons were set as linear and hyperbolic tangent sigmoid, respectively:

$$\varphi(net_j) = net_j \tag{6}$$

$$\varphi(net_j) = \frac{2}{1 + e^{-2net_j}} - 1 \tag{7}$$

The first is the identity function, and the latter takes the *net* values in the range $(-\infty, \infty)$ and converts it into an output in the interval (-1, 1).

The neural network toolbox provided by MATLAB-2016a was used to develop the model. A multilayer perceptron (MLP) network with one hidden layer was used to form the ANN architecture. Adjusting the weight to ensure the desired output, based on experimental data, is defined as the training process. Given the acceptable performance in solving problems related to concrete materials (Duan et al., 2017) the back-propagation learning algorithm (Werbos 1994) was employed to train the system. This learning process consists of two main steps:

(1) A forward flow of the input signal from the input layer toward the output layer and a calculation of error based on the comparison between the network's output and the target value, i.e. experimental data. The cost function (error) to be minimized (with respect to the ANN weights w) is given by:

$$J(w) = \frac{1}{2N} \sum_{i=1}^{N} [y_i - \hat{y}_i]^2 \tag{8}$$

where $\hat{y}_i = f(x_i, w)$ is the output of the neural network when using a training set comprised of N samples of {input, output} pairs: $\mathcal{T} = \{x_i, y_i\}_{i=1}^{N}$.

(2) Backward propagation of the error signal and an adjustment of all the neurons' weights to minimize the error according to the generalized delta rule:

$$w^{new} = w^{old} + \Delta w^{old} \tag{9}$$

In this work, the optimization method of Levenberg-Marquardt backpropagation (LMBP) was used to train the MLP (Levenberg, 1944, Marquardt 1963) since it is well-known to be effective (Hagan 1994, Fu et al., 2015, Haykin, 2009):

$$\Delta w = [H + \mu I]^{-1} g \tag{20}$$

$$g = \nabla_w J(w) = \frac{\partial J(w)}{\partial w} \tag{21}$$

$$H = \nabla^2{}_w J(w) = \frac{\partial^2 J(w)}{\partial w^2} \tag{22}$$

where μ is a regularizing parameter; g and H are the gradient and Hessian of the cost function $J(w)$; and I is the identity matrix. If the cost function increases, the regularizing parameter is increased by a factor of μ^+, otherwise it is decreased by μ^- and the generalized delta rule is applied to update the weights.

Early stopping criterion based on consecutive validation set error checks were used to avoid overfitting the training data and to allow a better generalization performance of the MLP for previously unseen data. Additionally, each input parameter was scaled to the range (-1, 1).

In this study, a genetic algorithm (GA) (Eiben & Smith 2007) with integer representation was used to tune the internal parameters of the MLP, specifically, the number of hidden neurons, the maximum number of validation checks, the initial regularizing parameter value, and its increase and decrease ratios.

A total of 436 data samples, corresponding to 90% of the data available in the developed database, were randomly selected for training the neural network. The 43 data series obtained from laboratory investigations (discussed in Section 2.2.) were used for model validation. The remaining 10% of the data from the database were used for testing the selected model.

The GA optimization was carried out using a population of 100 individuals for 100 generations. To measure the performance consistency of a given ANN parameter configuration, the fitness function of the GA was defined as the median of the validation mean square error (MSE) of a given parameter configuration after the realization of 30 trials, each of which with random weight initialization (to address the local optima issues common to these types of neural networks).

36

The ANN parameters optimized using GA included the number of hidden neurons (N) within the range of [1, 30] and 30 grid points, the maximum number of validation checks (V) within the range of [3, 10] and 8 grid points, the initial regularizing parameter (μ) within the range of [0.001,1] and 1000 grid points, the regularizing parameter decrease ratio (μ^-) within the range of [0.1, 0.8] and 100 grid points, and the regularizing parameter increase ratio (μ^+) within the range of [1.5, 10] and 100 grid points. These parameters were discretized using a grid of linearly and equally spaced points within their respective ranges from which the GA was used to evolve the best combination. The optimization toolbox provided by MATLAB-2016a was used to perform this parameter tuning. The following fixed parameters were considered during the GA optimization: LMBP training method and MSE cost function were used, respectively. The maximum training time was fixed at 1s while the maximum number of epochs was 10^2. The performance goal was 0, with a minimum gradient of 10^{-7}, and the maximum regularizing parameter (μ_{max}) of 10^3.

The GA was run 10 times and the solutions obtained were used in the next step of the model development, which consisted of running 1000 trials for each of the ANN parameter configurations and selecting the one with the best performance in terms of the validation set error. In case of a tie, the architecture with the best training error was selected. For fine-tuning purposes, an additional parameter sweep analysis of the number of hidden neurons was carried out by fixing the other parameters around values close to the solutions obtained by the GA. This setting of the number of neurons in the MLP's hidden layer is related to the approach discussed by Duan et al. (2017), in which the number of neurons is varied and the best architecture is selected. Finally, the same procedure was performed with an equal set of default parameters for all scenarios. The selected parameters are listed in Table 13.

Table 13 - ANN parameters when performing the hidden layer parameter sweep analysis

| Parameter description | Parameter value per scenario (GA) | | | | Default parameters |
| | Number of parameters | | | | |
	13	18	15	21	
Training method	LMBP	LMBP	LM P	LMBP	LMBP
Cost function	MSE	MSE	MSE	MSE	MSE
Number of hidden neurons (N)	7	7	28	16	(11, 8, 10, 8)
Maximum number of validation checks (V)	9	9	7	6	10
Initial regularizing parameter (μ)	0.7	0.14	0.03	0.03	0.001
Regularizing param. decrease ratio (μ^{-})	0.2	0.26	0.50	0.14	0.1
Regularizing param. increase ratio (μ^{+})	2.4	2.8	2.70	5.10	10
Maximum regularizing param. (μ_{max})	10^{10}	10^{10}	10^{10}	10^{10}	10^{10}

The performance metrics, i.e. regression results and MSE summarizing the correlations between the estimated values (neural network's output) and the experimental data (target values), of all the ANNs after the parameter tuning process are listed in Table 14. For each case, the optimal ANN parameter configuration for the training, validation, and test subsets were incorporated as defined earlier to investigate the different subsets of features including 13, 15, 18 or 21 input parameters. Strong correlations were observed for the investigated models. The obtained correlation (R) values ranged from 0.71 to 0.95 for the training phase, 0.86 to 0.92 for the validation phase, and 0.74 to 0.89 for the testing phase. The MSE values ranged from 0.00140 to 0.00690 for the training, 0.00128 to 0.00218 for the validation, and 0.00359 to 0.00848 for the testing phases. The Bold values indicate best performance across train, validation, and test sets in Table 14.

Table 14 - Summary of the performance of various models

Scenario	R			MSE		
	Train.	Valid.	Test	Train.	Valid.	Test
After the hidden layer parameter sweep analysis and using the remaining parameter values close to GA solutions						
(I) 13 Features	**0.9287***	0.8634	**0.8906**	**0.00187**	0.00218	**0.00359**
(II) 18 Features	0.9389	**0.9193**	**0.8332**	0.00161	0.00196	**0.00571**
(III) 15 Features	0.7098	**0.9123**	0.8092	0.00690	**0.00155**	0.00620
(IV) 21 Features	**0.9396**	0.9086	0.8460	**0.00160**	0.00142	0.00511
After a hidden neurons parameter sweep analysis using default parameters						
(I) 13 Features**	0.9259	**0.8750**	0.8861	0.00194	**0.00193**	0.00382
(II) 18 Features	**0.9472**	0.8959	0.7410	**0.00140**	**0.00159**	0.00848
(III) 15 Features	**0.9298**	0.8794	**0.8846**	**0.00184**	0.00180	**0.00382**
(IV) 21 Features	0.9138	**0.9175**	**0.8677**	0.00225	**0.00128**	**0.00424**

*Bold values indicate the best performance across train, validation and test sets
**Selected model

6.4 MODEL SELECTION

The results presented in Table 14 suggest that the MLP is robust with respect to the parameter selection for this specific function approximation problem. Additionally, in terms of minimum MSE and the correlation coefficient (R), the prediction performances of the four models regarding their respective scenarios seem comparable. Therefore, based on Occam's razor (Duda et al., 2000), i.e. the principle of parsimony, the simplest model was selected: Scenario I with default parameters due to the smaller validation error. In other words, given the requirements for proper prediction are met, it is generally recommended to select regression models with a lower number of input parameters. It is also recommended to avoid dependent variables as input parameters to avoid multi-collinearity, unless it is proven that the incorporation of such features can enhance the model performance.

Figure 9 presents the correlations between the neural network's predictions about the selected model and the experimental values obtained during training, validation, and testing along with their respective MSEs. Figure 10 depicts the MLP prediction and the experimental value of the R_{MOE} side by side for each sample. A reasonable match was obtained between the model predictions and the experimental values of R_{MOE}, especially considering that the training data consisted of a collection of samples from technical publications (with case-by-case variations in experimental procedures, instruments, and conditions) with missing values that still needed to be estimated; yet the ANN performs reasonably well in the validation (population of laboratory experiments) and in the test set. This fact indicates that the MLP is an adequate modeling tool for this estimation problem.
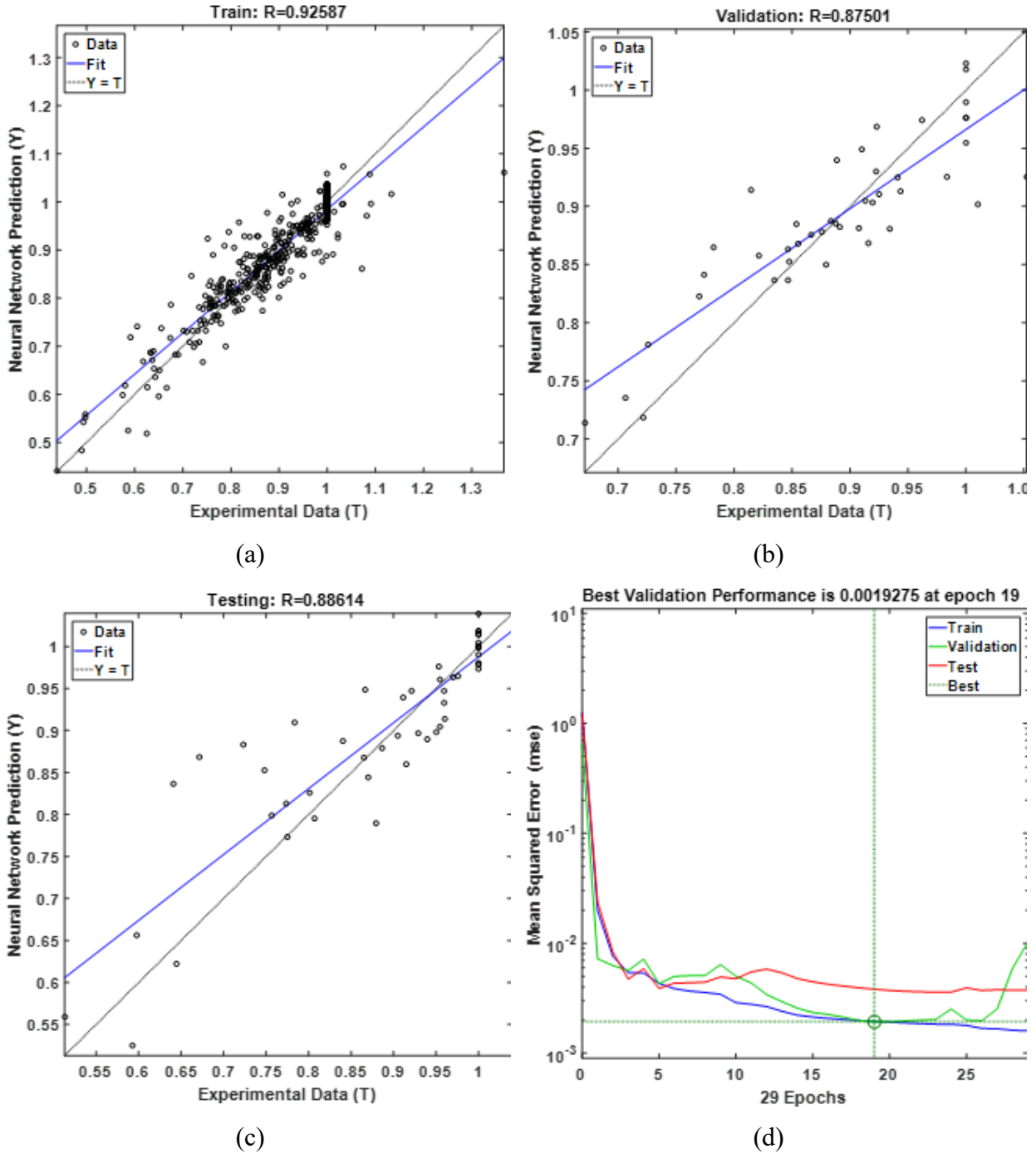
Figure 9 - ANN model performance with 13 input parameters (Scenario I). The correlation coefficient between the experimental values and the ANN predictions for training (a), validation (b), and testing (c) is shown. The MSE during training, validation, and testing is depicted in (d) as a function of the training epochs (one epoch corresponds to an entire pass through the training data samples).
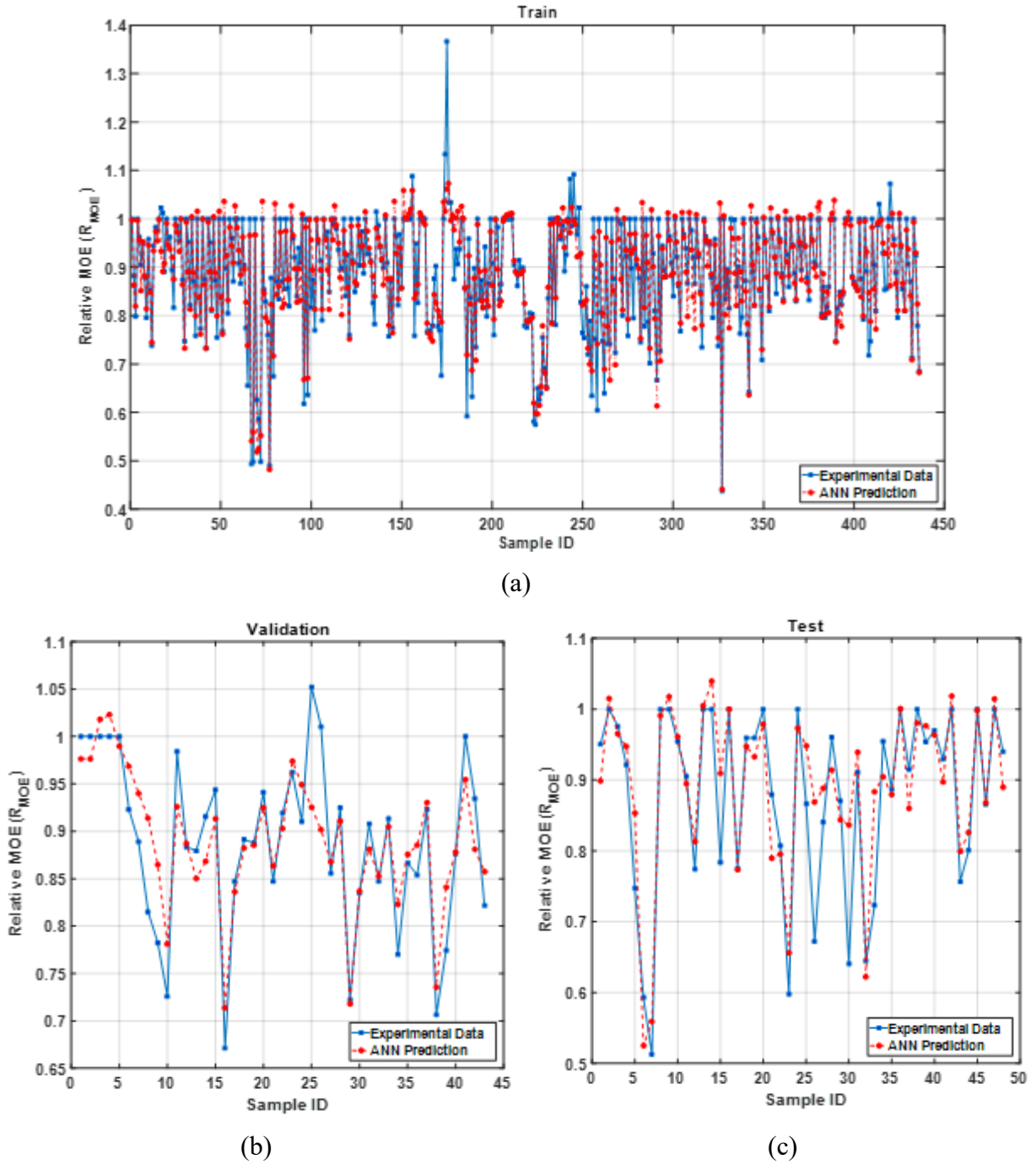
(a)

(b)

(c)

Figure 10 - The ANN model prediction (Scenario I with default parameters) and experimental data for the training (a), validation (b) and testing (c) versus their respective input indices (Sample ID).

6.5 CASE STUDY: RIGID PAVEMENT WITH MODOT REFERENCE CONCRETE

The model will be applicable to a wide range of applications, as long as the input parameters are within the range of the database used for model development. Given the fact that transportation infrastructure is one of the main potential markets for RCA consumption, the selected model was employed to quantify the effect of RCA on the MOE of concrete for rigid pavement construction. The test scenario involved investigating the rate of variation in the MOE of concrete prepared with 545 lb/yd^3 (323 kg/m^3) of cementitious materials and 0.40 w/cm. The simulated mixture was made with virgin coarse aggregate with 0.8% water absorption, 4602 lb/yd^3 (2730 kg/m^3) specific gravity, and 28% LA abrasion mass loss. The range of the investigated RCA properties were: (1) water absorption of 1.8% - 8.5%, oven-dry specific gravity of 3540 - 4214 lb/yd^3 (2100 - 2500 kg/m^3), and a replacement rate of 0 to 100% (by mass) for the simulation according to Scenario I. It should be noted that the mixture design and material properties used for case study are well within the typical criteria for rigid pavement construction used by state departments of transportations (Sadati and Khayat 2016).

Figure 11 presents the effect of RCA water absorption and the replacement rate (% mass) on the extent of variation in the MOE based on the model investigated in Scenario I. In general, the results indicate a reduction in the MOE due to the use of RCA with higher water absorption. The rate of reduction in the MOE was limited to 10% when RCA with water absorption limited to 2.5% was used (even up to 100% replacement). The rates of reduction in the MOE were 10%, 15%, and 20%, respectively, when 30%, 50%, and 100% RCA with water absorption of 4% were used in pavement concrete. The reduction rates were 15%, 20%, and 40%, respectively, when 30%, 50%, and 100% RCA with water absorption of 6% were used.

Figure 12 presents the effect of RCA oven dry specific gravity on the rate of variation in the MOE at different replacement ratios (% mass). In general, a reduction in MOE was observed as a result of using RCA with a lower oven dry specific gravity. However, the reduction in the MOE was limited to 10% when RCA with an oven dry specific gravity higher than 156 lb/ft³ (2500 kg/m³) was used. The results presented in Figure 12 indicate a 15%, 25%, and 45% reduction in the MOE when 30%, 50%, and 100% RCA with an oven dry specific gravity of 137 lb/ft³ (2200 kg/m³) was used in pavement concrete. The rates of reduction in the MOE were 15%, 20%, and 30% when 30%, 50%, and 100% RCA with an oven dry specific gravity of 143.6 lb/ft³ (2300 kg/m³) were used. The results presented in Figure 11 and Figure 12 also revealed that the use of 30% and 50% RCA can lead to a reduction of up to 20% and 30% in the MOE of pavement concrete when low-quality RCA with an oven dry specific gravity of 131 lb/ft³ (2100 kg/m³) and water absorption as high as 8.5% were used.
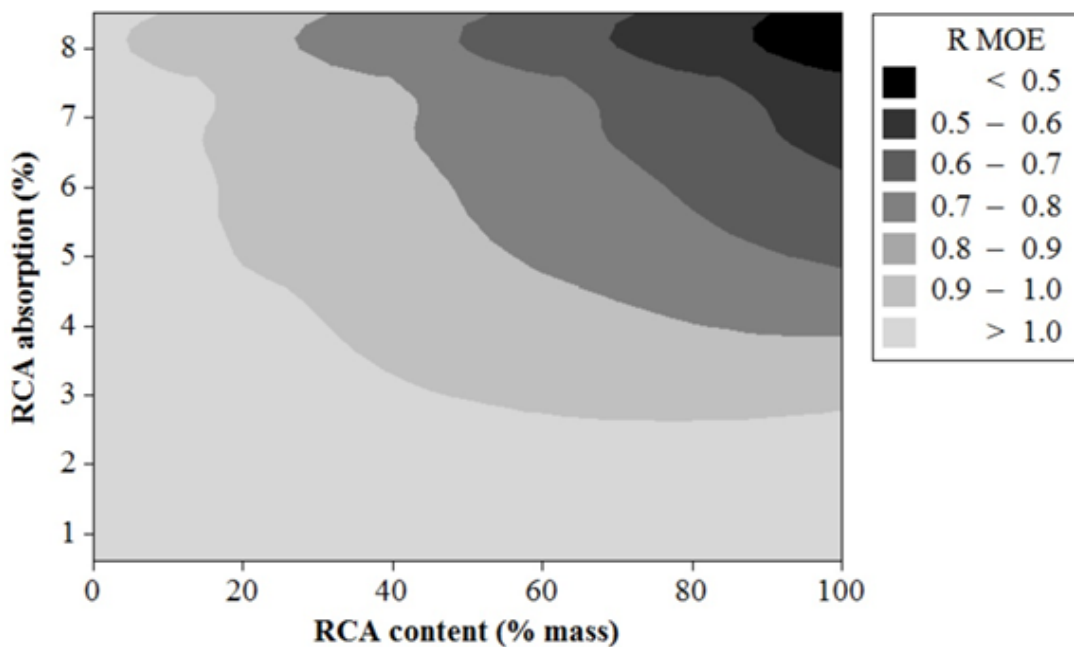

Figure 11 - Effect of RCA water absorption on MOE of concrete designated for rigid pavement construction, Scenario I
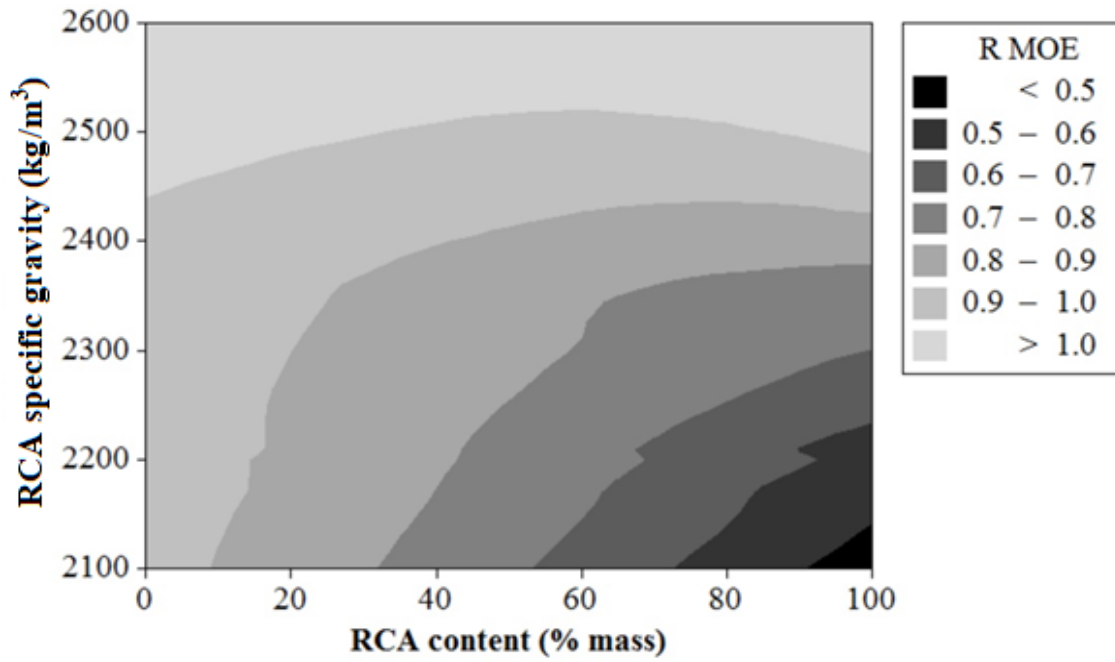
Figure 12 - Effect of RCA oven dry specific gravity on MOE of concrete designated for rigid

pavement construction, Scenario I

7. CONCLUSIONS AND RECOMMENDATIONS

The test results from the study demonstrate the feasibility of using RCA and high-volume SCMs for the production of sustainable concrete mixtures in transportation infrastructure. This included the replacement of cement with at least 50% SCMs and the aggregate with 50% RCA. Nine optimized mixtures from the first phase of the project that exhibited satisfactory performance were selected for single layer and two-lift concrete pavement systems. The mixtures optimized for use in single layer pavement or for the top layer of two-lift concrete pavement exhibited 91-day compressive strength greater than 6,600 psi (45.5 MPa), 56-d flexural strength greater than 720 psi (5.0 MPa), 90-d drying shrinkage lower than 450 $\mu\varepsilon$, and freeze-thaw durability factor of over 90%. The mixtures optimized for the bottom layer of the two-lift concrete pavement exhibited 91-day compressive strength greater than 7,100 psi (49.0 MPa), 56-d flexural strength greater than 740 psi (5.1 MPa), 90-d drying shrinkage lower than 490 $\mu\varepsilon$, and frost durability factor of 96%.

Life cycle cost assessment indicated that sustainable concrete with optimal SCMs and RCA content can lead to cost savings of 17.6% of agency costs, 12.1% of user cost, 12.1% of social cost, and 17.5% of total life cycle cost.

Given the variability of the properties of RCA and its effect on mechanical properties, the water absorption, specific gravity, and LA abrasion mass loss of RCA were found to be effective means to classify RCA sources. Lowering the water absorption and LA abrasion mass loss values and increasing the oven dry specific gravity of RCA can lead to higher quality of the aggregate and greater mechanical properties of the concrete made with such RCA.

The data obtained through the case study indicate that the reduction in the MOE of pavement concrete can be limited to 10% when the coarse RCA with water absorption lower than 2.5%, LA abrasion less than 23%, or oven dry specific gravity higher than 156 lb/ft^3 (2500 kg/m^3)

is used, even at a full replacement rate. The use of 30% and 50% RCA can lead to a reduction of up to 20% and 30% in the MOE of pavement concrete, respectively, when a relatively low-quality RCA is selected that has an oven dry specific gravity of 131 lb/ft^3 (2100 kg/m^3) and a water absorption as high as 8.5%.

REFERENCES

American Concrete Pavement Association (ACPA) (2008), Recycled Concrete in Subbases: a Sustainable Choice, Technical Series, TS204.9P, ACPA, Washington, D.C. [Online]. Available: http://www.pavement.com/Concrete_Pavement/Technical/Downloads/TSs.asp.

ASTM C39, (2001). Standard Test Method for Compressive Strength of Cylindrical Concrete Specimens.

ASTM C143, (2015). Standard Test Method for Slump of Hydraulic-Cement Concrete.

ASTM C231, (2014). Standard Test Method for Air Content of Freshly Mixed Concrete by The Pressure Method.

ASTM C469/C469M, (2010). Standard Test Method for Static Modulus of Elasticity and Poisson's Ratio of Concrete in Compression.

ASTM C1202, (2018). Standard Test Method for Electrical Indication of Concrete's Ability to Resist Chloride Ion Penetration.

CDOT (2016). Colorado Department of Transportation Pavement Design Manual.

Choi, S., and Won, M., (2009), Performance of Continuously Reinforced Concrete Pavement Containing Recycled Concrete Aggregate, Geohunan International Conference on New Technologies in Construction and Rehabilitation of Portland Cement Concrete Pavement and Bridge Deck Pavement, ASCE.

Cuttel, D., Snyder, M., Vandenbossche, J., and Wade, M., (1997), Performance of Rigid Pavements Containing Recycled Concrete Aggregates, Transportation Research Record 1574, Transportation research board, Washington D.C.

Duan, Z., Poon, C.S., and Xiao, J. (2017). Using Artificial Neural Networks to Assess the Applicability of Recycled Aggregate Classification by Different Specifications. Materials and Structures, 50(2), 107.

Duda, R.O., Hart, P.E., and Stork, D.G. (2000). Pattern Classification, 2nd ed. Hoboken, NJ, USA: Wiley.

Eiben, A.E., and Smith, J.E. (2007). Introduction to Evolutionary Computing. Publisher: Springer-Berlin.

Englesen, C., Mehus, J., Pade, C., and Saether, D., (2005), Carbon Dioxide Uptake in Demolished and Crushed Concrete, Project Report 395-2005, Norwegian Building Research Institute, Oslo, Norway.

Federal Highway Administration (2004), Transportation Applications of Recycled Concrete Aggregate, FHWA State of the Practice National Review.

Fu, X., Li, S., Fairbank, M., and Wunsch, D.C., and Alonso, E. (2015). Training Recurrent Neural Networks with the Levenberg - Marquardt Algorithm for Optimal Control of a Grid-Connected Converter. IEEE Transactions on Neural Networks and Learning Systems, 26(9), 1900-1912.

Gabr, A.R., and Cameron, D.A., (2012), Properties of Recycled Concrete Aggregate For Unbound Pavement Construction, Journal of Materials in Civil Engineering, 24, 754-764.

Garber, S., Rasmussen, R., Cackler, T., Taylor, P., Harrington, D., Fick, G., Snyder, M., Van Dam, T., and Lobo, C., (2011), A Technology Development Plan for the Use of Recycled Concrete Aggregates in Concrete Paving Mixtures, National Concrete Pavement Technology Center.

González-Taboada, I., González-Fonteboa, B., Martínez-Abella, F., and Carro-López, D. (2016). Study of Recycled Concrete Aggregate Quality and its Relationship with Recycled Concrete Compressive Strength Using Database Analysis. Materiales De Construcción, 66(323), 089.

Hagan, M.T., and Menhaj, M.B. (1994). Training Feedforward Networks with the Marquardt Algorithm. IEEE Trans. Neural Netw., 5(6), 989-993.

Haykin, S., (2009). Neural Networks and Learning Machines, Pearson Education, Upper Saddle River, NJ.

Khayat, K.H., and Sadati, S. (2016). High-Volume Recycled Materials for Sustainable Pavement Construction. Final Report, Missouri Department of Transportation (No. cmr17-006).

Kim. K., Shin. M., and Soowon, Cha, (2013), Combined Effects of Recycled Aggregate and Fly Ash Towards Concrete Sustainability, Construction and Building Materials, 48, 499-507.

Levenberg, K., (1944). A Method for the Solution of Certain Non-Linear Problems in the Least Squares. Quart. J. Appl. Math., 2(2), 164-168.

Marquardt, D.W., (1963). An algorithm for Least-Squares Estimation of Nonlinear Parameters. J. Soc. Ind. Appl. Math., 11(2), 431-441.

Mclntyre. J., Spatari. S., and MacLean. H.L., (2009), Energy and Greenhouse Gas Emissions Trade-offs of Recycled Concrete Aggregate Use in Nonstructural Concrete: A North American Case Study, Journal of Infrastructure Systems, 15, 361-370.

MODOT (2004). Pavement Design and Type Selection Process Phase I Report.

Omary, S., Ghorbel, E., and Wardeh, G. (2016). Relationships between Recycled Concrete Aggregates Characteristics and Recycled Aggregates Concrete Properties. Construction and Building Materials, 108, 163-174.

Padmini, A.K., Ramamurthy, K., Mathews, M.S., (2009), Influence of Parent Concrete on the Properties of Recycled Aggregate Concrete, Construction and Building Materials, 23(2), 829-836.

Sadati, S., and Khayat, K.H., (2016). Field Performance of Concrete Pavement Incorporating Recycled Concrete Aggregate. Construction and Building Materials, 126, 691-700.

Sadati, S., Enzo Brito da Silva, L., Wunsch, D., and Khayat, K.H. (2019). Artificial Intelligence to Investigate Modulus of Elasticity of Recycled Aggregate Concrete, ACI Materials Journal, 116(1), 51-62.

Salas, A., Lange, D., Roesler J., (2010), Batching Effects on Properties of Recycled Aggregate Concrete for Airfield Rigid Pavements, FAA Technology Transfer Conference and Exposition, Atlantic City, NJ, USA.

Surya, M., Rao, K.V., and Lakshmy, P., (2013), Recycled Aggregate Concrete for Transportation Infrastructure, Procedia - Social and Behavioral Sciences, 104, 1158-1167.

Tam, V.W.Y., Gao, X.F., Tam, C.M., (2005), Microstructural Analysis of Recycled Aggregate Concrete Produced from Two-Stage Mixing Approach, Cement and Concrete Research, 35, 1195-1203.

Werbos, P.J., (1994). The Roots of Backpropagation: From Ordered Derivatives to Neural Networks and Political Forecasting (Vol. 1). John Wiley & Sons.